Biochemistry

 Volume 38, Number 36 September 7, 1999

Accelerated Publications

FTIR Study of the Primary Electron Donor of Photosystem I (P700) Revealing Delocalization of the Charge in $P700^+$ and Localization of the Triplet Character in $^3P700$

Jacques Breton,* Eliane Nabedryk, and Winfried Leibl

Section de Bioénergétique, Département de Biologie Cellulaire et Moléculaire, CEA/Saclay, 91191 Gif-sur-Yvette, France

Received May 27, 1999; Revised Manuscript Received July 19, 1999

ABSTRACT: The effect of global ^{15}N or ^2H labeling on the light-induced $P700^+/P700$ FTIR difference spectra has been investigated in photosystem I samples from *Synechocystis* at 90 K. The small isotope-induced frequency shifts of the carbonyl modes observed in the $P700^+/P700$ spectra are compared to those of isolated chlorophyll *a*. This comparison shows that bands at 1749 and 1733 cm^{-1} and at 1697 and 1637 cm^{-1}, which upshift upon formation of $P700^+$, are candidates for the 10a-ester and 9-keto C═O groups of P700, respectively. A broad and relatively weak band peaking at 3300 cm^{-1}, which does not shift upon global labeling or $^1H-^2H$ exchange, is ascribed to an electronic transition of $P700^+$, indicating that at least two chlorophyll *a* molecules (denoted P_1 and P_2) participate in $P700^+$. Comparisons of the $^3P700/P700$ FTIR difference spectrum at 90 K with spectra of triplet formation in isolated chlorophyll *a* or in RCs from photosystem II or purple bacteria identify the bands at 1733 and 1637 cm^{-1}, which downshift upon formation of $^3P700$, as the 10a-ester and 9-keto C═O modes, respectively, of the half of P700 that bears the triplet (P_1). Thus, while the P_2 carbonyls are free from interaction, both the 10a-ester and the 9-keto C═O of P_1 are hydrogen bonded and the latter group is drastically perturbed compared to chlorophyll *a* in solution. The Mg atoms of P_1 and P_2 appear to be five-coordinated. No localization of the triplet on the P_2 half of P700 is observed in the temperature range of 90−200 K. Upon P700 photooxidation, the 9-keto C═O bands of P_1 and P_2 upshift by almost the same amount, giving rise to the 1656(+)/1637(−) and 1717(+)/1697(−) cm^{-1} differential signals, respectively. The relative amplitudes of these differential signals, as well as of those of the 10a-ester C═O modes, appear to be slightly dependent on sample orientation and temperature and on the organism used to generate the $P700^+/P700$ spectrum. If it is assumed that the charge density on ring V of chlorophyll *a*, as measured by the perturbation of the 10a-ester or 9-keto C═O IR vibrations, mainly reflects the spin density on the two halves of the oxidized P700 special pair, a charge distribution ranging from 1:1 to 2:1 (in favor of P_2) is deduced from the measurements presented here. The extreme downshift of the 9-keto C═O group of P_1, indicative of an unusually strong hydrogen bond, is discussed in relation with the models previously proposed for the PSI special pair.

In the reaction centers (RCs)[1] of all photosynthetic organisms, light promotes electron transfer from the singlet excited state of a chlorophyllic primary electron donor (P) to a series of cofactors that serve as sequential electron

* To whom correspondence should be addressed: SBE/DBCM, Bât. 532, CEA/Saclay, 91191 Gif-sur-Yvette Cedex, France. Telephone: (331) 69 08 22 39. Fax: (331) 69 08 87 17. E-mail: cadara3@dsvidf.cea.fr.

[1] Abbreviations: PSI (II), photosystem I (II); RC, reaction center; B(Chl), bacterio(chlorophyll); P, primary electron donor; P_1 and P_2, primary electron donor Chls constituting P700; F_A, F_B, and F_X, FeS terminal electron acceptors; THF, tetrahydrofuran; FTIR, Fourier transform infrared.

10.1021/bi991216k CCC: $18.00
Published on Web 08/20/1999

acceptors. The resulting charge-separation process occurs with a near-unity quantum yield. Because of their obvious relevance to the understanding of photoinduced separation and stabilization of charges in photosynthetic systems, the structure of P and P^+ has been the subject of sustained interest. In purple bacteria, P is a dimer of bacteriochlorophyll (BChl) molecules whose structure in the neutral, cation, and triplet states has been investigated by various spectroscopic techniques and for which structural models at a resolution up to 2.3 Å have been determined for the ground state (*1*−*3*). Although the crystal structure of photosystem I (PSI) has been determined (*4*, *5*), the present 4 Å resolution is not yet sufficient to provide a detailed view of the structure of the primary donor (P700). However, the crystallographic data concur with previous results from optical (*6*−*10*) and resonance Raman (*11*) spectroscopy to show that P700 is a dimer of chlorophyll *a* (Chl *a*). Furthermore, EPR spectroscopy has long been used to investigate the electronic structure of $P700^+$. Although, initially, a dimeric state of $P700^+$ with approximately equal spin sharing on the two Chl molecules was proposed (*12*, *13*), this conclusion has been questioned (*14*, *15*). More recent ENDOR and ESEEM experiments with frozen solutions and crystals of PSI have favored a dimer of Chl *a* with a decidedly asymmetrical spin density distribution ranging from 3:1 to 10:1 (*16*−*20*). The latest report concludes that the unpaired spin is completely localized on a single Chl (*21*). Thus, the extent of the asymmetry of $P700^+$ remains ambiguous. Other important open questions concern the localization of the spin density in the ^{3}P700 triplet state (*22*−*24*) and the identification of the axial Mg ligands to P700 and $P700^+$ (*25*−*29*).

Vibrational spectroscopy is well suited to addressing the participation of one or two Chl *a* molecules in P700, $P700^+$, and ^{3}P700 and to exploring the interactions of these molecules with the protein. An intense 1717(+)/1700(−) cm^{-1} differential signal in the light-induced FTIR difference spectra of P700 photooxidation has been interpreted in terms of the frequency upshift upon cation formation of the 9-keto carbonyl of one or two Chl *a* molecule(s) constituting P700 (*30*−*34*). The high frequency of the 9-keto mode shows that this group is free from interaction with the protein. In contrast, on the basis of resonance Raman spectroscopy, it has been proposed that the 9-keto group of each of the two Chl *a* molecules in P700 is hydrogen bonded, although to different extents (*11*). The electronic coupling of the two molecules in the cation state of P can be probed in the mid-IR by investigating electronic transitions corresponding to hole exchange between the two halves of the oxidized dimer (*35*−*41*). Compared to the large magnitude of the P^+ electronic transition in purple bacteria, green bacteria, and heliobacteria, the apparent lack of a defined band of $P700^+$ in the 2000−2800 cm^{-1} frequency range has notably been taken as evidence of a monomeric state of $P700^+$ (*32*, *34*). Furthermore, comparison of the FTIR difference spectra corresponding to the generation of either the cation state or the triplet state of primary electron donors constitutes a sharp tool with which to ascertain the vibrational modes of the neutral state of P. This approach, which was initially applied to purple bacteria and has allowed the vibrational frequency of the 9-keto C═O group of each of the two BChl *a* molecules in the P870 dimer to be determined (*42*), has not yet been utilized for P700. In the case of photosystem II (PSII), where the monomeric, dimeric, or multimeric nature of the primary donor P680 is still debated (*43*), the FTIR difference spectrum of a so-called "^{3}P680" state has been reported (*44*). Comparison with the FTIR difference spectrum of $P680^+$ showed unambiguously that this triplet state could not reside on any one of the Chl molecules that constitute P680 (*41*, *45*).

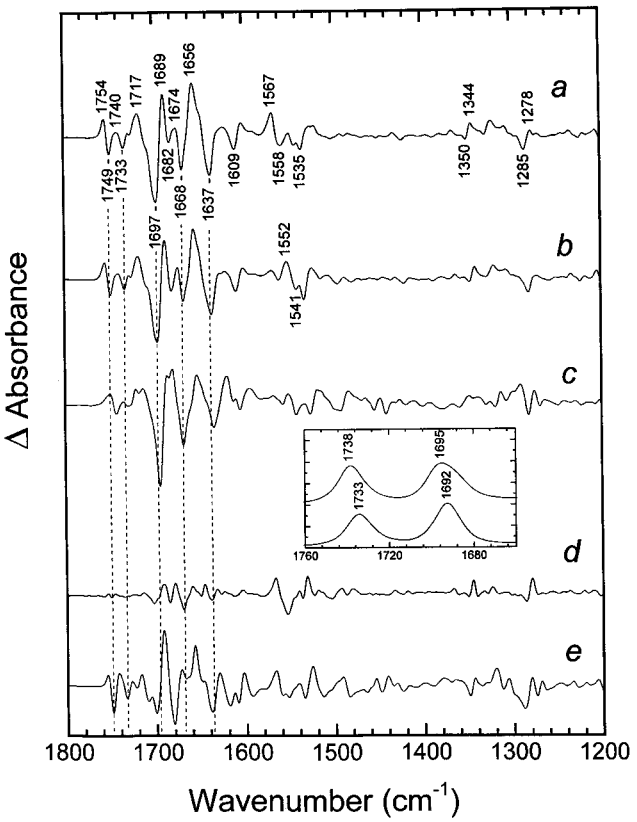

FIGURE 1: Light-induced $P700^+$/P700 FTIR difference spectra of films of PSI particles from *Synechocystis* at 90 K: (a) unlabeled PSI, (b) ^{15}N-labeled PSI, and (c) ^{2}H-labeled PSI. Double-difference spectra are displayed as traces d (^{14}N-minus-^{15}N) and e (^{1}H-minus-^{2}H). In trace a, the peak-to-peak amplitude is 5×10^{-4} absorbance unit. In traces a−c, about 100 000 interferograms were added. In the inset are shown IR absorbance spectra of Chl *a* in THF at 290 K: (top) unlabeled Chl *a* and (bottom) ^{2}H-labeled Chl *a*. The frequency of the bands is given ±1 cm^{-1}. The spectral resolution was 4 cm^{-1}.

In view of the many questions that are still pending with regard to the electronic structure and bonding interactions of P700, we have examined the effect of global ^{15}N or ^{2}H labeling as well as of ^{1}H−^{2}H exchange on the low-temperature $P700^+$/P700 FTIR difference spectra. We also have analyzed the mid-IR region corresponding to a possible electronic transition of $P700^+$ and have studied the triplet state ^{3}P700. The results lead us to conclude that P700 is a dimer of two Chl *a* molecules that differ drastically in the hydrogen bonding state of their 9-keto carbonyl group. A definite sharing of the hole over the two molecules is found in $P700^+$. Our low-temperature data also show a complete localization of the triplet state on the P700 Chl with the most perturbed (downshifted) carbonyl.

MATERIALS AND METHODS

PSI particles from *Synechocystis* sp. PCC 6803 were prepared according to the method described in ref *46*.

Extraction of F_A and F_B was performed by urea treatment (*47*), and removal of F_X was achieved following the method described in ref *48*. Depletion of the FeS centers was verified by the disappearance of slow (millisecond) phases of reduction of $P700^+$ by back-reactions with these terminal electron acceptors, as determined from the flash-induced absorption change at 820 nm (*47*, *48*). Uniformly labeled PSI samples were prepared by growing the cells either in ^2H_2O or in the presence of ^{15}N-labeled sodium nitrate. The extent of labeling was >95% for ^{15}N samples (P. Sétif, personal communication) and >99% for ^2H samples (N. Gilles, personal communication).

Films were prepared by spreading 20 μL of a suspension of PSI particles (2 mg of Chl *a*/mL) containing trehalose (10 mM), sodium ascorbate (5 mM), and phosphate buffer (5 mM, pH 8.5) on a CaF_2 window (25 mm diameter) and drying under argon. To generate $^3P700$, the film was covered with 5 μL of sodium dithionite (1 M) in phosphate buffer (1 M, pH 8.5). The sample was then illuminated at 20 °C for 10 mn with strong white light before being cooled to low temperatures. The FTIR difference spectra were recorded on a Nicolet 60 SX or Magna 860 spectrometer, as previously described (*32*, *42*).

RESULTS

$P700^+$/P700 FTIR Difference Spectra. The light-induced FTIR difference spectra measured at 90 K on films of purified PSI preparations from *Synechocystis* are depicted in the 1800−1200 cm^{-1} frequency range for an unlabeled sample (Figure 1a) and for samples uniformly labeled with either ^{15}N (Figure 1b) or ^2H (Figure 1c).[2] The spectrum of the unlabeled sample is essentially identical to that reported previously (*32*) except for the improved S/N ratio. Although we have observed, as discussed below, that these spectra contain small contributions from the FeS centers, we will term these spectra $P700^+$/P700 for simplicity.

The impact on the $P700^+$/P700 spectra of the uniform labeling with ^{15}N, which is best followed by comparing the direct spectra (Figure 1a,b) to the double-difference ^{14}N-minus-^{15}N spectrum (Figure 1d), is quite small and is mostly localized under the main amide I (1700−1625 cm^{-1}) and amide II (1570−1520 cm^{-1}) bands. The 1567(+)/1558(−) cm^{-1} differential signal in the spectrum of the unlabeled PSI (Figure 1a) downshifts by 15 cm^{-1} in the ^{15}N-labeled sample (Figure 1b) as does the amide II band (60% N−H bending, 40% C−N stretching) in the absorption spectrum (not shown). The differential signals under the amide I band (80% peptide C═O stretching) can be assigned to the small coupling between the peptide C═O stretching and N−H bending modes which is also responsible for the downshift from 1656 to 1653 cm^{-1} of the amide I band. Below 1500 cm^{-1}, several negative bands with small amplitudes, notably, at 1350 and 1285 cm^{-1}, correspond closely to Chl *a* bands in the cation-minus-neutral difference spectrum (*31*). These bands exhibit a 3−4 cm^{-1} downshift upon ^{15}N labeling and are due to coupled skeletal C−C, C−H, and C−N modes of the Chl molecule(s) of P700 (*50*). Note that the two large differential signals at 1717/1697 and 1656/1637 cm^{-1} of the $P700^+$/P700 spectrum are not much affected by ^{15}N labeling (Figure 1a,b,d). These differential signals are also practically unperturbed upon extensive $^1H-^2H$ exchange (not shown).

When uniform ^2H labeling is employed, the differential feature at 1754(+)/1749(−) cm^{-1} downshifts by 5 cm^{-1} while the two negative bands at 1697 and 1637 cm^{-1} downshift by 2 cm^{-1} (Figure 1a,c). In addition, pronounced perturbations of the spectrum are observed around 1680 cm^{-1} and under the amide II band, while the negative band at 1668 cm^{-1} appears to upshift by 1 cm^{-1}. In the case presented here, where the purified PSI samples isolated from cells grown in ^2H_2O were prepared in ^1H_2O, the frequency shifts observed in the region of absorption of the C═O modes (Figure 1a,c) cannot be due to exchangeable protons. These shifts are ascribed to the effect of ^2H labeling on vibrations from either the protein or the Chl *a* that are coupled to nonexchangeable N−H, O−H, or C−H modes. If the negative bands at 1697 and 1637 cm^{-1}, which exhibit a 2 cm^{-1} downshift upon ^2H labeling, were to be assigned to peptide C═O modes or to side chain C−N or NH_2 modes, they should also downshift upon ^{15}N labeling. As such a shift is not observed (Figure 1a,c,d), we are led to propose that the two large negative bands at 1697 and 1637 cm^{-1} are rather to be assigned to Chl *a* 9-keto C═O vibrations. This proposal is strengthened by comparing the effect of ^2H labeling on the Chl *a* carbonyl vibrations in situ and in vitro. When ^2H labeling is employed, the IR bands of the ester and 9-keto C═O vibrations of isolated Chl *a* in tetrahydrofuran (THF) also exhibit downshifts of 5 and 3 cm^{-1}, respectively (inset of Figure 1), while they are unaffected by ^{15}N labeling (not shown). The 5 cm^{-1} shift of the 10a-ester C═O is explained by the proximity of hydrogen atoms at C_{10} and on the methyl of the carbomethoxy group, while the smaller shift of the 9-keto C═O is likely to be due to the coupling of the 10a-ester and 9-keto C═O modes.

$^3P700$/P700 FTIR Difference Spectra. When the FeS acceptors are prereduced or absent, illumination of purified PSI samples under reducing conditions usually generates the $^3P700$ triplet state (*51*). Under the specific conditions of the FTIR experiments, which require a thin film of a concentrated sample, we have only been able to generate a mixture of $^3P700$ and $P700^+$ upon addition of sodium dithionite to films of intact PSI. However, complete removal of the FeS centers allows the $^3P700$ state to be largely populated under steady state illumination, most probably because of double reduction of the phylloquinone acceptor A_1 (*51*).

The $^3P700$/P700 FTIR difference spectrum recorded at 90 K (Figure 2a) is dominated by a prominent differential signal negative at 1637 cm^{-1} and positive at 1594 cm^{-1} with a shoulder at 1585 cm^{-1}. This signal is absent in control samples containing 100 mM ferricyanide (not shown). When $^3P700$/P700 spectra recorded on reduced samples from different batches of FeS-depleted preparations are compared, there is a slight variability in the relative intensities of some small signals above 1690 cm^{-1}, notably, for the negative band

[2] The high S/N ratio needed to investigate the effect of isotopic substitution requires extensive signal averaging over long periods of time. Therefore, working at low temperatures was found to be most suitable. The spectra that are shown (Figure 1a−c) correspond to the fraction of the $P700^+FeS^-$ state that can be reversibly populated under steady state saturating illumination at 90 K. In view of the quasi-irreversibility of the charge separation in a fraction of the RCs at low temperatures (*49*), the amplitude of the measured absorption changes typically represents 25% of the amplitude of the signal obtained on the first cycle of illumination after cooling the sample in the dark. However, the spectra of the reversible and irreversible $P700^+FeS^-$ states are identical within the noise level.

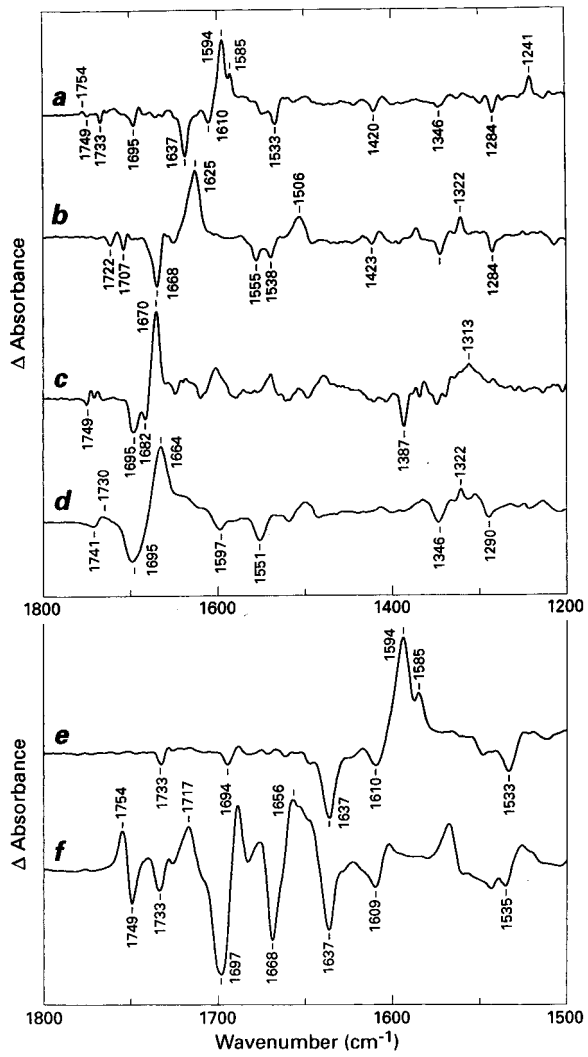

FIGURE 2: Light-induced triplet-minus-singlet FTIR difference spectra. (a) ^{3}P700/P700 spectrum of PSI particles from *Synechocystis* at 90 K, (b) "^{3}P680/P680" spectrum of spinach PSII RCs at 10 K, (c) ^{3}P870/P870 spectrum of *Rb. sphaeroides* RCs at 85 K, and (d) ^{3}Chl *a*/Chl *a* spectrum of Chl *a* in THF at 90 K. The peak-to-peak amplitudes are 5, 3, 1, and 7×10^{-4} absorbance unit for traces a−d, respectively. Traces e and f are comparisons of the corrected (see the text) ^{3}P700/P700 (e) and P700$^+$/P700 (f) spectra.

at 1695 cm^{-1} and, most specifically, for a very small 1754(+)/1749(−) cm^{-1} differential signal. The latter signal is observed consistently but varies in amplitude from sample to sample. This observation suggests that the experimental triplet spectrum (Figure 2a) could be contaminated by a small amount of the P700$^+$ state. Two additional observations support this view. Upon the intensity of the actinic light being decreased, the magnitudes of the bands assigned to P700$^+$/P700 increase relative to those of ^{3}P700/P700 (not shown). The relative contribution of the P700$^+$/P700 bands also increases upon raising the temperature, with the ^{3}P700 contribution becoming vanishingly small at 200 K. These observations are consistent with the different lifetimes and temperature dependencies of the P700$^+$F$_X^-$ and ^{3}P700 states (*51*, *52*). Accordingly, the experimental spectrum was corrected by subtracting a fraction (2−5%) of the P700$^+$/P700 signal to eliminate the small residual 1754(+)/1749(−) cm^{-1} differential signal in Figure 2a. The calculated ^{3}P700/P700 spectrum (Figure 2e) is very close to the experimental one and exhibits small bands at 1733 and 1694 cm^{-1}. When uniform ^{2}H labeling is employed, the negative band at 1733 cm^{-1} downshifts by 6 cm^{-1} while those at 1694 and 1637 cm^{-1} downshift by 1−2 cm^{-1} (not shown).

The ^{3}P700/P700 spectrum offers definite similarities to the so-called "^{3}P680" state generated by white light illumination of isolated PSII RCs at cryogenic temperatures (Figure 2b; *44*; J. Breton, unpublished[3]), to the previously reported ^{3}P870/P870 spectrum of the primary electron donor of *Rhodobacter sphaeroides* at 85 K (*42*; Figure 2c), and to the ^{3}Chl/Chl FTIR difference spectrum at 90 K of Chl *a* in THF (*44*, *53*; Figure 2d). All these triplet spectra exhibit one or two small differential features in the region of absorption of the 10a-ester C═O (1760−1700 cm^{-1}) and a larger one in the absorption range of the 9-keto C═O (1700−1640 cm^{-1}). The shape of these differential features demonstrates a downshift of the carbonyl frequencies upon triplet formation. This is the opposite of the upshift of the carbonyls observed upon cation formation (*31*). It is interesting to note that the IR frequencies of the 9-keto C═O of the BChl *a* molecules in P870 (Figure 2c), which are known to be free from bonding interaction with the RC protein (*2*), are very little downshifted compared to those of the 9-keto C═O of isolated Chl *a* in THF (Figure 2d), while one 9-keto C═O mode of Chl *a* in P700 (Figure 2a) is drastically downshifted.

Mid-IR Electronic Transition of P700$^+$. In previous studies (*32*, *34*), a significant amplitude of the P700$^+$ electronic transition of *Synechocystis* in the 2800−2000 cm^{-1} mid-IR range could not be detected. Above 2000 cm^{-1}, broad signals with small amplitudes are difficult to measure reliably because the steep decline of the spectral sensitivity of the MCT detectors can lead to a nonlinear response and to skewed baselines. These difficulties are compounded by the intense absorption of water in the 3700−3000 cm^{-1} frequency range where the amide A mode (N−H stretching at 3300 cm^{-1}) also absorbs. Since the above-mentioned studies, the conditions for sample preparation have been optimized to maximize the amplitude and reversibility of the light-induced IR changes (*38*, *54*). Furthermore, a new setup based on a DTGS detector with a highly linear response between 200 and 10000 cm^{-1} has been implemented (*55*). These technical improvements led us to reexamine the P700$^+$/P700 spectrum in the mid-IR region extended up to 5000 cm^{-1}.

A typical P700$^+$/P700 FTIR difference spectrum in the frequency range of 5000−1000 cm^{-1} of *Synechocystis* at 90 K (Figure 3a) exhibits a roof-shaped signal extending between 4500 and 2000 cm^{-1} and peaking around 3300 cm^{-1}. This signal is found at a significantly higher energy and with a lower extinction coefficient than the analogous P$^+$ bands previously observed in purple and green bacteria and heliobacteria (*32*, *35*−*40*) as well as in PSII (*41*; J. Breton, unpublished). The shape and amplitude of the broad P700$^+$

[3] While the spectrum in Figure 2b has been recorded at 10 K, the ones recorded between 85 and 150 K are very close to those reported in ref *44*. Note, however, that the 1707 cm^{-1} band is still present at 10 K. This is incompatible with the model and assignments proposed in ref *44*.

[4] The small changes observed in the amide I and amide II regions when comparing the light-induced difference spectra obtained for pairs of samples prepared with and without methyl viologen are assigned to contributions from the FeS centers (W. Leibl and J. Breton, unpublished results). It has also been determined that these IR signals have no significant effect on the position and amplitude of the bands assigned to 9-keto C═O vibrations of Chl *a*.

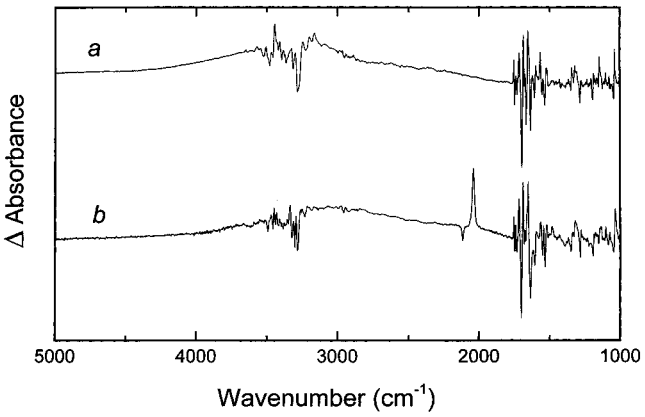

FIGURE 3: Comparison of the $P700^+$/P700 FTIR difference spectra of PSI particles from (a) *Synechocystis* in dry film at 90 K and (b) spinach in a paste containing 50 mM ferricyanide and 450 mM ferrocyanide at 280 K.

mid-IR transition are not appreciably affected when the temperature is raised from 90 (Figure 3a) to 280 K (not shown). To investigate the possibility that the FeS centers could be responsible for a significant fraction of the broad transition, methyl viologen was added to the samples to accept electrons from the photoreduced FeS centers (*39*). The addition of this compound does not alter the shape of the broad transition appreciably.[4] The effect of ^{2}H or ^{15}N labeling on the sharp differential signals in the 3500−3100 cm^{-1} range (Figure 3a) leads to their assignment to N−H and O−H stretching vibrations of inaccessible groups in the interior of the protein that surrounds P700. On the other hand, the broad underlying $P700^+$ transition remains unaffected by ^{1}H−^{2}H exchange or by ^{2}H and ^{15}N substitution.

To ascertain whether the broad mid-IR transition of $P700^+$ observed in *Synechocystis* is specific to this species or is a more general characteristic of $P700^+$, purified PSI samples from spinach have also been investigated. A representative spectrum is shown in Figure 3b for a sample evaluated at 280 K in the presence of a mixture of ferricyanide (50 mM) and ferrocyanide (450 mM). The former compound accepts electrons from the reduced FeS centers as documented by the signs of the ferricyanide and ferrocyanide IR signals at 2116 and 2036 cm^{-1}, respectively (Figure 3b). Under such conditions, it is possible to perform light-minus-dark cycles over several days without significant degradation of the $P700^+$/P700 spectrum, and thus, the highly linear, but less sensitive, DTGS detector can be used. The broad mid-IR transition of $P700^+$ is indeed present (Figure 3b). The slight differences in the shape and peak position compared to measurements with *Synechocystis* at 280 K apparently are genuine, as they could also be fully reproduced with the same sample using the MCT detector. Comparison of the spectra (Figure 3) to those previously reported highlights the importance of both the improved S/N ratio and the extension of the frequency range up to 5000 cm^{-1} in obtaining a reliable profile of the broad mid-IR transition of $P700^+$. Consideration of the actual spectra (Figure 3) in the spectral range up to 2800 cm^{-1} only would be insufficient for assessing whether a new band exists.

DISCUSSION

FTIR Evidence That P700 Is a Dimer of Chl a. The investigation of the photooxidation of P700 by FTIR spectroscopy reported here provides several lines of evidence that both P700 and $P700^+$ should be considered as a dimer of Chl *a*. First, comparison of the $P700^+$/P700 spectra (Figure 1a) with the electrochemically induced (pyro)Chl a^+/(pyro)-Chl *a* spectra in THF (*31*) allows us to recognize characteristic IR signatures of the formation of Chl a^+ species in $P700^+$. This has previously led to assignment of the 1754/1749 and 1733/1740 cm^{-1} differential signals to the upshift of the 10a-ester C═O groups of the Chl(s) upon P700 photooxidation and assignment of the 1717/1697 cm^{-1} differential signal to an upshift of the 9-keto C═O group(s) (*31*, *32*). The observation that the effects of ^{2}H or ^{15}N isotope substitution on the carbonyl bands of the neutral species are very similar for Chl *a* in THF and in P700 strongly supports these assignments. Second, $P700^+$ exhibits a broad mid-IR band. This band, being unaffected by ^{2}H or ^{15}N labeling or ^{1}H−^{2}H exchange, cannot be vibrational in nature and is thus ascribed to an electronic transition of $P700^+$ (*35*, *36*). This implies that at least two Chl *a* molecules share the charge. Third, the $P700^+$/P700 spectrum (Figure 1a) exhibits additional negative bands that are possible candidates for carbonyl groups of another Chl *a* molecule contributing to P700. While one band at 1733 cm^{-1}, which downshifts by 6 cm^{-1} upon ^{2}H labeling, is likely to be the 10a-ester C═O mode of the second Chl *a* molecule, two negative bands at 1668 and 1637 cm^{-1} are potential contenders for the corresponding 9-keto C═O group. The 1668 cm^{-1} band is variable from species to species and is temperature-dependent. It is affected neither by ^{1}H−^{2}H exchange nor by ^{15}N substitution and is slightly upshifted upon ^{2}H labeling, which is uncharacteristic of a Chl *a* molecule. On the other hand, the behavior of the 1637 cm^{-1} band upon isotope substitution is that expected for a 9-keto C═O group of Chl *a*. Although such a low frequency would be atypical for a 9-keto C═O group, its apparent upshift to 1656 cm^{-1} upon $P700^+$ formation is consistent with the properties of a Chl *a* cation. Finally, the ^{3}P700/P700 FTIR difference spectrum (Figure 2e) confirms that the 9-keto C═O group of one of the Chl *a* molecules in P700 absorbs at 1637 cm^{-1}. Compared to the cation state of P700 where the charges are liable to affect vibrations of the protein, the triplet state is electrically neutral and is thus a much gentler probe of the C═O vibrations of P700.

Comparison of the ^{3}P700/P700 and $P700^+$/P700 spectra (Figure 2e,f) shows that the band profile of the negative feature at 1637 cm^{-1} in the ^{3}P700/P700 spectrum fits precisely into the negative band at the same frequency of the $P700^+$/P700 spectrum (Figure 2e,f). This observation, together with the IR signature given by the unusual low frequency of this band, provides compelling evidence that the 9-keto C═O of the same Chl *a* molecule contributes to both spectra. In the analogous comparison between the P^+/P and ^{3}P/P spectra of P870, the same close correspondence of the frequency of the negative bands in the two spectra has led to the identification of the 9-keto C═O modes of P870 (*42*). On the other hand, the negative 9-keto C═O band observed at 1668 cm^{-1} in the spectrum of the so-called "^{3}P680/P680" triplet in PSII RCs (Figure 2b) is located right under a positive band of the $P680^+$/P680 spectrum, indicating that this triplet state is not localized on one of the Chl *a* molecules bearing the positive charge in $P680^+$ (*41*, *45*). Comparison of the ^{3}P700/P700 and $P700^+$/P700 spectra

further shows that the 10a-ester C═O vibration of the Chl *a* molecule that bears the triplet and exhibits the 9-keto mode at 1637 cm^{-1} (denoted in the following as P_1) absorbs at 1733 cm^{-1}. The second Chl *a* molecule in P700 (denoted as P_2) exhibits its 9-keto and 10a-ester C═O modes at 1697 and 1749 cm^{-1}, respectively.[5] The isotope shifts observed for the various carbonyl bands are fully consistent with these assignments. However, our assignments cannot be reconciled with those from resonance Raman spectroscopy (*11*).

Spin Density Distribution in ^{3}P700 and P700$^+$. With the assignments of the vibrational frequencies of the 9-keto and 10a-ester carbonyls of each of the two Chl *a* molecules constituting P700, the spin distribution in ^{3}P700 and in P700$^+$ can be discussed from the IR point of view. The ^{3}P700/P700 spectrum at 90 K exhibits no evidence of a triplet signature other than that of P_1, and there is no sign of delocalization of the triplet on another Chl *a* molecule at higher temperatures (up to 200 K). An asymmetry of the hydrogen bonding of the 9-keto C═O groups of the two halves of P700 could affect the relative energies of the triplet states of the two molecules in ^{3}P700, leading to the localization of the triplet character on one molecule. Note that, while the FTIR data presented here provide compelling evidence that ^{3}P700 is localized on a single Chl *a* molecule, it was not possible to discriminate by magnetic resonance between a true monomer and a dimer with parallel Chl planes (*22*, *23*).

Upon P700$^+$ formation, the 1697 cm^{-1} band of P_2 upshifts by 20 cm^{-1} while the 1637 cm^{-1} band of P_1 upshifts by 19 cm^{-1}. This value is comparable to the value of 25 cm^{-1} reported for the oxidation of isolated Chl *a* (*31*), indicating that the rate of exchange of the hole moving back and forth between P_1 and P_2 is slower than the 10^{-13} s resolution time of vibrational spectroscopy. The comparable 60 cm^{-1} frequency difference between the 9-keto C═O bands of P_1 and P_2 in both P700 and P700$^+$ indicates that the carbonyls probably do not change their interaction with the environment upon photooxidation of P700. Because of the comparable 20 cm^{-1} upshift upon photooxidation of the two 9-keto C═O groups, the peak-to-peak amplitude of the 1717/1697 and 1656/1637 cm^{-1} differential signals can be used as a crude estimate of the charge distribution on the two 9-keto C═O groups. This amplitude is somewhat smaller for P_1 than for P_2, especially for dried films at low temperatures. A more symmetrical charge distribution is usually observed at 280 K (not shown). The asymmetry also decreases when wet films or pastes are used instead of dried films, which suggests that orientation effects could play a role. This asymmetry might further be somewhat species-dependent, as indicated by the nearly equal amplitude of the 1717/1700 and 1654/1636 cm^{-1} differential signals obtained with a hydrated PSI sample from spinach (Figure 3b) and also as suggested by analyzing the various P700$^+$/P700 FTIR difference spectra reported in the literature (*28*, *30*−*34*). If the same extinction coefficient is assumed for the two 9-keto carbonyls, a global analysis of all our P700$^+$/P700 spectra provides an amplitude ratio varying from 1:1 to 2:1 in favor of the Chl *a* half bearing the 9-keto C═O absorbing at 1697 cm^{-1} (i.e., P_2). Note that the differential features of the 10a-ester C═O bands also provide comparable ratios, especially at higher temperatures (*28*, *30*, *34*). Thus, the extent of charge distribution in P700$^+$ is probed nearly equally well by the IR absorption changes of the two carbonyl groups of ring V (although they are perturbed very differently in P_1 and P_2). Assuming that the charge distribution between the two halves of P700$^+$ is reflected by the charge density on ring V, which is fully conjugated to the Chl *a* macrocycle, we arrive at a charge distribution ranging between 1:1 and 2:1 in favor of P_2. Although this proposal of a strong delocalization of the positive charge over the two halves of the P700$^+$ dimer agrees well with the early interpretations of ESR and ENDOR data (*12*, *13*), it is not consistent with the more recent conclusions derived from advanced magnetic resonance techniques (*16*−*21*).

FTIR Structural Model of P700. The evidence from FTIR that two Chl *a* molecules constitute the P700 special pair of PSI agrees with previous spectroscopic observations (*6*−*10*). It also agrees with the crystallographic model of PSI that shows two stacked macrocycles with their plane parallel to the membrane normal (*4*, *5*). This geometry is similar to that of the special pair in purple bacteria (*1*−*3*). Furthermore, linear dichroism of the flash-induced P700$^+$/P700 absorbance changes in the 600−800 nm spectral range measured on magnetically oriented chloroplasts provides a ratio of the amplitude of the high- and low-energy exciton components of P700 (*7*) that is close to that in bacterial RCs. Thus, the angle between the *Y*-axis of P_1 and P_2 must also be close to the corresponding value (30−35°) in bacterial RCs.

The IR frequencies of 1749 and 1697 cm^{-1} determined for the 10a-ester and 9-keto C═O groups of P_2, respectively, are typical for free carbonyls. On the other hand, the band of P_1 at 1733 cm^{-1} corresponds to a bound 10a-ester C═O, while that at 1637 cm^{-1} is indicative of an unusually large perturbation of a 9-keto C═O group such as that induced by a very strong hydrogen bond. The Chl *a* modes present at around 1610 and 1535 cm^{-1} in the ^{3}P700/P700 and P700$^+$/P700 spectra (Figure 2e,f) are marker bands for a five-coordinated Mg atom (*56*). The absence of six-coordinated Mg marker bands at around 1600 and 1515 cm^{-1} in the P700$^+$/P700 spectrum indicates that each of the Chl *a* molecules in P700 has probably only one axial ligand. With regard to the nature of the axial ligands to the Mg atoms of P_1 and P_2, ESEEM data for *Synechocystis* PSI with isotopically labeled histidines have been interpreted in terms of one His residue that is coordinated to the Mg atom of P700$^+$ (*26*). In view of the dimeric state of P700$^+$ derived from the study presented here, this conclusion should probably be modified to include the possibility of spectrally identical His axial ligands to the Mg atoms of both P_1 and P_2. Indeed, a recent search for potential axial ligands to the chlorophylls of P700, based on targeting all the conserved His residues present at homologous positions in both PsaA and PsaB subunits, has identified PsaA-His676 and PsaB-His656 as the best candidates for binding the P700 special pair (*27*−*29*). It was notably found that mutations of these two residues were the only ones that elicited significant changes in the 1760−1600 cm^{-1} range of the P700$^+$/P700 FTIR difference spectra (*28*, *29*).

A possible clue to the nature of the interaction that leads to the extraordinarily low frequency of the 9-keto C═O of

[5] The small negative signal at 1694 cm^{-1} (Figure 2e) does not behave like a residual contribution from the P700$^+$/P700 state. It is rather tentatively assigned to the perturbation (decoupling) of the 9-keto C═O mode of P_2 when the triplet state localizes on P_1.

P_1 (1637 cm^{-1}) is given by the work of Katz and co-workers on the IR properties of aggregated forms of Chl *a* (*57*, *58*). Long ago, these authors reported that Chl *a* in hydrated aliphatic hydrocarbon solvents tends to form an oligomer exhibiting IR frequencies at 1727 and 1638 cm^{-1} for the 10a-ester and 9-keto C═O groups, respectively (*58*). The latter value is strikingly close to that of the 9-keto C═O of P_1 at 1637 cm^{-1}. It was further proposed that the oligomer consists of stacked Chl *a* molecules with a water molecule coordinated to the Mg atom of one Chl *a* molecule and hydrogen bonded to both the 9-keto and the 10a-ester C═O groups of the following Chl *a* molecule. The increased acidity of the water coordinated to Mg is thought to be responsible for the anomalous strength of the hydrogen bond to the 9-keto C═O group of Chl *a* (*59*). The 1638 cm^{-1} frequency appears to be characteristic of a 9-keto C═O interacting with a water molecule coordinated to the Mg atom of a Chl as such a low frequency for a 9-keto C═O group is observed neither upon direct coordination with the Mg atom of another Chl *a* molecule nor upon interaction with methanol or other nucleophilic compounds (*60*). Indeed, an X-ray diffraction study of ethyl chlorophyllide *a*·$2H_2O$ crystals showed the presence of water coordinated to the Mg atom of one molecule and hydrogen bonded to the 9-keto C═O group of another molecule (*61*). A second water molecule is hydrogen bonded to the coordinated water molecule and also to the 10a-ester C═O group of the other chlorophyllide. The near coincidence of the IR frequency of the 9-keto C═O of P_1 in P700 with that of the hydrated Chl *a* oligomers suggests that a water molecule may coordinate the Mg atom of P_2. However, such a model cannot be accommodated in a straightforward manner with the results of the spectroscopic effect of the mutations of PsaB-His656 and PsaA-His676 which indicate that these residues probably act as fifth ligand to the Mg atom of P_1 and P_2, respectively (*28*, *29*). Several other Chl *a* dimers ligated by water have also been proposed as models for P700 (*62*−*64*). However, they involved either translational symmetry or C_2 symmetry, notably, at the level of the carbonyl groups, which would further make them inconsistent with the FTIR results of P700 presented here.

One of the unique properties of the P700 special pair involves its redox properties as this primary donor possesses a midpoint potential about 400 mV lower than that of Chl *a* in vitro (necessary to avoid energy loss in the linear electron transport chain of oxygenic photosynthesis). In contrast, the primary donor of purple bacteria has a midpoint potential only about 200 mV lower than that of BChl *a* in solution, and P680 is some hundred millivolts more positive than Chl *a* in vitro. Specific alterations of the oxidation potential of P870 by interaction with the protein scaffold have been characterized in mutant RCs of *Rb. sphaeroides*. In particular, introduction of hydrogen bonds to the 9-keto or 2a-acetyl C═O groups leads to an increase in the redox potential of P870 by 60−125 mV per hydrogen bond (*65*). Thus, the low oxidation potential of P700 cannot be related directly to the unusual strength of a hydrogen bond that would be responsible for the observed frequency of 1637 cm^{-1} of the 9-keto C═O group of P_1. It is conceivable that the hydrogen bonds control only indirectly the redox potential of P, e.g., by influencing the conformation of the macrocycle which could be a main determinant of the midpoint potential. To rationalize the unusual redox potential and magnetic resonance properties of $P700^+$, a monomeric Chl *a* enol has been put forward as an alternative model to the P700 dimer (*66*). Enolization of the ring V β-keto ester of Chl *a* results in a very different π electronic structure of the macrocycle. The frequency of 1637 cm^{-1} observed for the 9-keto C═O group of P_1 is taken to indicate at least a partial enolization of ring V. One may propose that an unusually strong hydrogen bond, possibly even bifurcated hydrogen bonds, involving residues other than His could be responsible for such a perturbation of the 9-keto C═O group of P_1. Still another possibility involves Chl *a*′ (diastereoisomer of Chl *a* at C_{10}) whose conspicuous presence in the core of PSI (*67*) has always constituted a puzzle. Advances in the resolution of the crystal structure of PS I together with site-directed mutagenesis and additional FTIR experiments are needed to improve the current picture of the primary electron donor of PSI.

ACKNOWLEDGMENT

We thank Sandra Andrianambinintsoa, Emilie Counil, Dominique Dejonghe, Gérard Berger, Jacques Kléo, and Alain Valleix for sample preparation, Nicolas Gilles, Hervé Bottin, and Pierre Sétif for isotopically labeled cultures, and Claude Boullais and Bill Parson for stimulating discussions.

REFERENCES

1. Deisenhofer, J., Epp, O., Sinning, I., and Michel, H. (1995) *J. Mol. Biol. 246*, 429−457.
2. Allen, J. P., Feher, G., Yeates, T. O., Komiya, H., and Rees, D. C. (1987) *Proc. Natl. Acad. Sci. U.S.A. 84*, 5730−5734.
3. Ermler, U., Fritzsch, G., Buchanan, S. K., and Michel, H. (1994) *Structure 2*, 925−936.
4. Krauss, N., Schubert, W.-D., Klukas, O., Fromme, P., Witt, H. T., and Saenger, W. (1996) *Nat. Struct. Biol. 3*, 965−973.
5. Schubert, W.-D., Klukas, O., Krauss, N., Saenger, W., Fromme, P., and Witt, H. T. (1997) *J. Mol. Biol. 272*, 741−769.
6. Philipson, K. D., Sato, V. L., and Sauer, K. (1972) *Biochemistry 11*, 4591−4595.
7. Breton, J. (1977) *Biochim. Biophys. Acta 459*, 66−75.
8. den Blanken, H. J., and Hoff, A. J. (1983) *Biochim. Biophys. Acta 724*, 52−61.
9. Ikegami, I., and Itoh, S. (1988) *Biochim. Biophys. Acta 934*, 39−46.
10. Krawczyk, S., and Macsymiec, W. (1991) *FEBS Lett. 286*, 110−112.
11. Moënne-Loccoz, P., Robert, B., and Lutz, M. (1990) *Biochemistry 29*, 4740−4746.
12. Norris, J. R., Uphaus, R. A., Crespi, H. L., and Katz, J. J. (1971) *Proc. Natl. Acad. Sci. U.S.A. 68*, 625−628.
13. Norris, J. R., Scheer, H., Druyan, M. E., and Katz, J. J. (1974) *Proc. Natl. Acad. Sci. U.S.A. 71*, 4897−4900.
14. Wasielewski, M. R., Norris, J. R., Crespi, H. L., and Harper, J. (1981) *J. Am. Chem. Soc. 103*, 7664−7665.
15. O'Malley, P. J., and Babcock, G. T. (1984) *Proc. Natl. Acad. Sci. U.S.A. 81*, 1098−1101.
16. Davis, I. H., Heathcote, P., MacLachlan, D. J., and Evans, M. C. W. (1993) *Biochim. Biophys. Acta 1143*, 183−189.
17. Rigby, S. E. J., Nugent, J. H. A., and O'Malley, P. J. (1994) *Biochemistry 33*, 10043−10050.
18. Evans, M. C. W., Bratt, P. J., Heathcote, P., and Moënne-Loccoz, P. (1995) in *Photosynthesis: from Light to Biosphere* (Mathis, P., Ed.) Vol. II, pp 183−186, Kluwer, Dordrecht, The Netherlands.
19. Käss, H., and Lubitz, W. (1996) *Chem. Phys. Lett. 251*, 193−203.
20. Käss, H., Fromme, P., and Lubitz, W. (1996) *Chem. Phys. Lett. 257*, 197−206.

21. Mac, M., Bowlby, N. R., Babcock, G. T., and McCracken, J. (1998) *J. Am. Chem. Soc. 120*, 13215−13223.
22. Frank, H. A., McLean, M. B., and Sauer, K. (1979) *Proc. Natl. Acad. Sci. U.S.A. 76*, 5124−5128.
23. Rutherford, A. W., and Sétif, P. (1990) *Biochim. Biophys. Acta 1019*, 128−132.
24. Sieckmann, I., Brettel, K., Bock, C., van der Est, A., and Stehlik, D. (1993) *Biochemistry 32*, 4842−4847.
25. Cui, L., Bingham, S. E., Khun, M., Käss, H., Lubitz, W., and Webber, A. N. (1995) *Biochemistry 34*, 1549−1558.
26. Mac, M., Tang, X.-S., Diner, B. A., McCracken, J., and Babcock, G. T. (1996) *Biochemistry 35*, 13288−13293.
27. Webber, A. N., Su, H., Bingham, S. E., Käss, H., Krabben, L., Khun, M., Jordan, R., Schlodder, E., and Lubitz, W. (1996) *Biochemistry 35*, 12857−12863.
28. Redding, K., McMillan, F., Leibl, W., Brettel, K., Hanley, J., Rutherford, A. W., Breton, J., and Rochaix, J.-D. (1998) *EMBO J. 17*, 50−60.
29. Leibl, W., Brettel, K., Nabedryk, E., Breton, J., Rochaix, J.-D., and Redding, K. (1998) in *Photosynthesis: Mechanisms and Effects* (Garab, G., Ed.) Vol. I, pp 595−598, Kluwer, Dordrecht, The Netherlands.
30. Tavitian, B. A., Nabedryk, E., Mäntele, W., and Breton, J. (1986) *FEBS Lett. 201*, 151−157.
31. Nabedryk, E., Leonhard, M., Mäntele, W., and Breton, J. (1990) *Biochemistry 29*, 3242−3247.
32. Nabedryk, E., Leibl, W., and Breton, J. (1996) *Photosynth. Res. 48*, 301−308.
33. MacDonald, G., Bixby, K. A., and Barry, B. A. (1993) *Proc. Natl. Acad. Sci. U.S.A. 90*, 11024−11028.
34. Hamacher, E., Kruip, J., Rögner, M., and Mäntele, W. (1996) *Spectochim. Acta A52*, 107−121.
35. Breton, J., Nabedryk, E., and Parson, W. W. (1992) *Biochemistry 31*, 7503−7510.
36. Parson, W. W., Nabedryk, E., and Breton, J. (1992) in *The Photosynthetic Bacterial Reaction Center II* (Breton, J., and Verméglio, A., Eds.) pp 79−88, Plenum Press, New York.
37. Nabedryk, E., Allen, J. P., Taguchi, A. K. W., Williams, J. C., Woodbury, N. W., and Breton, J. (1993) *Biochemistry 32*, 13879−13885.
38. Nabedryk, E., Breton, J., Williams, J. C., Allen, J. P., Kuhn, M., and Lubitz, W. (1998) *Spectrochim. Acta A54*, 1219−1230.
39. Noguchi, T., Kusumoto, N., Inoue, Y., and Sakurai, H. (1996) *Biochemistry 35*, 15428−15435.
40. Noguchi, T., Fukami, Y., Oh-oka, H., and Inoue, Y. (1997) *Biochemistry 36*, 12329−12336.
41. Noguchi, T., Tomo, T., and Inoue, Y. (1998) *Biochemistry 37*, 13614.
42. Breton, J., and Nabedryk, E. (1993) *Chem. Phys. Lett. 213*, 571−575.
43. Diner, B. A., and Babcock, G. T. (1996) in *Oxygenic Photosynthesis: The Light Reactions* (Ort, D. R., and Yocum, C. F., Eds.) pp 213−247, Kluwer, Dordrecht, The Netherlands.
44. Noguchi, T., Inoue, Y., and Satoh, K. (1993) *Biochemistry 32*, 7186−7195.
45. Breton, J., Hienerwadel, R., and Nabedryk, E. (1997) in *Spectroscopy of Biological Molecules: Modern Trends* (Carmona, P., Navarro, R., and Hernanz, A., Eds.) pp 101−102, Kluwer, Dordrecht, The Netherlands.
46. Bottin, H., and Sétif, P. (1991) *Biochim. Biophys. Acta 1057*, 331−336.
47. Golbeck, J. H., Parrett, K. G., Mehari, T., Jones, K. L., and Brand, J. J. (1988) *FEBS Lett. 228*, 268−272.
48. Warren, P. V., Golbeck, J. H., and Warden, J. T. (1993) *Biochemistry 32*, 849−857.
49. Ke, B., Demeter, S., Zamaraev, K. I., and Khairutdinov, R. F. (1979) *Biochim. Biophys. Acta 545*, 265−284.
50. Lutz, M., and Mäntele, W. (1991) in *Chlorophylls* (Scheer, H., Ed.) pp 855−902, CRC Press, Boca Raton, FL.
51. Sétif, P., Hervo, G., and Mathis, P. (1981) *Biochim. Biophys. Acta 638*, 257−267.
52. Golbeck, J. H., and Cornelius, J. M. (1986) *Biochim. Biophys. Acta 849*, 16−24.
53. Breton, J., and Nabedryk, E. (1993) in *Spectroscopy of Biological Molecules* (Theophanides, T., Anastassopoulou, J., and Fotopoulos, N., Eds.) pp 309−310, Kluwer Academic Publishers, Dordrecht, The Netherlands.
54. Breton, J., and Nabedryk, E. (1998) *Photosynth. Res. 55*, 301−307.
55. Breton, J., Nabedryk, E., and Clerici, A. (1999) *Vib. Spectrosc. 19*, 71−75.
56. Fujiwara, M., and Tasumi, M. (1986) *J. Phys. Chem. 90*, 5646−5650.
57. Katz, J. J., Ballschmiter, K., Garcia-Morin, M., Strain, H. H., and Uphaus, R. A. (1968) *Proc. Natl. Acad. Sci. U.S.A. 60*, 100−107.
58. Ballschmiter, K., and Katz, J. J. (1969) *J. Am. Chem. Soc. 91*, 2661−2677.
59. Zundel, G., and Murr, A. (1967) *Z. Phys. Chem. 54*, 49−58.
60. Cotton, T. M., Loach, P. A., Katz, J. J., and Ballschmiter, K. (1978) *Photochem. Photobiol. 27*, 735−749.
61. Strouse, C. E. (1974) *Proc. Natl. Acad. Sci. U.S.A. 71*, 325−328.
62. Wasielewski, M. R., Norris, J. J., Shipman, L. L., Lin, C.-P., and Svec, W. A. (1981) *Proc. Natl. Acad. Sci. U.S.A. 78*, 2957−2961.
63. Fong, F. K. (1974) *Proc. Natl. Acad. Sci. U.S.A. 71*, 3692−3695.
64. Shipman, L. L., Cotton, T. M., Norris, J. R., and Katz, J. J. (1976) *Proc. Natl. Acad. Sci. U.S.A. 73*, 1791−1794.
65. Allen, J. P., and Williams, J. C. (1995) *J. Bioenerg. Biomembr. 27*, 275−283.
66. Wasielewski, M. R., Studier, M., and Katz, J. J. (1976) *Proc. Natl. Acad. Sci. U.S.A. 73*, 4282−4286.
67. Maeda, H., Watanabe, T., Kobayashi, M., and Ikegami, I. (1992) *Biochim. Biophys. Acta 1099*, 74−80.

BI991216K